# The Effect of Electron Donor and Withdrawing Groups Attached to 1,2,3-Selendiazole Based Compounds on Anti-Cancer Properties

Usman Sani MUHAMMAD[1]*, (iD) Sultan ERKAN[1]

[1] *Department of Chemistry, Faculty of Science, Sivas Cumhuriyet University, Sivas 58140, Turkey*

*Corresponding author: U. S. MUHAMMAD (YYY@gmail.com)*

## ABSTRACT

The optimized structure of 1,2,3-selendiazole based compounds 9c, 9c-1 and 9c-2 was obtained at the B3LYP/6-31G+(d) level. Quantum parameters such as the highest occupied molecular orbital energy ($E_{HOMO}$), the lowest unoccupied molecular orbital energy ($E_{LUMO}$), the energy gap ($\Delta E$), hardness ($\eta$), softness ($\sigma$), electronegativity ($\chi$), chemical potential ($\mu$), global molecular electrophilicity index ($\omega$), global molecular nucleophilicity index ($\varepsilon$), the electron accepting ($\omega^+$) and electron donating ($\omega^-$) powers were compared for investigated molecules. Different from 9c, the effects of ethyl and chloro substituents on 1,2,3-selendiazole were examined. It has been found that ethyl and chlorine substituents change their inhibition activities according to their electron donating properties. Molecular electrostatic potential maps and frontier molecular orbital contour diagrams of the investigated compounds were obtained at the calculation level. Electrophilic and nucleophilic regions were determined for 9c, 9c-1 and 9c-2. The studied compounds were docked against a breast cancer (MCF7) cell line to investigate the antitumor activities. Molecular docking results were found to be higher than 9c-2 against MCF-7 cell line.

## 1. INTRODUCTION

Selenium is an essential trace element for the human body and some animals to sustain life. Organo-selenium compounds have some excellent properties such as high bioavailability, strong bioactivity, low toxicity, anti-oxidation, anti-inflammatory and anti-cancer [1-3]. Epidemiological, preclinical and clinical studies support the role of selenium compounds as potent cancer chemopreventive agents [4,5]. Selenium supplementation has been found to be effective in reducing the incidence of cancers including prostate, lung, colon and liver cancers [6]. In recent years, various mechanisms have been proposed to elucidate the anticancer activity of selenium, including induction of cell apoptosis or cell cycle arrest, inhibition of cell proliferation, modulation of the redox state, detoxification of the carcinogen, stimulation of the immune system, and inhibition of angiogenesis. [5]. Recent studies have shown that selenium holds promise as an agent that can reduce the harmful side effects of radiotherapy. Clinical evaluations using various selenium doses have shown a significant reduction in chemotherapy and radiotherapy toxicity [7]. Selenadiazoles are important heterocyclic compounds containing two nitrogen atoms and one selenium. Selenium atom is named differently depending on its position in the ring. There are four types of selenadiazole, such as 1,2,3-selenadiazole (C-Se-N-N bond), 1,2,4-selenadiazole (N-C-Se-N) bond, 1,2,5-selenadiazole (N-C-Se-C-N) and 1,3,4-selenadiazole (N-Se-N). Atta et al. synthesized 1,2,3-selena-diazolofurochromones in 2010 and examined their anticancer activity. The synthesized 1,2,3-selena-diazolofurochromones in 2010 and examined their anticancer activity. In these synthesis studies, 9c was found to be the most active compound against the MCF-7 tumor cell line [8].

In this study, we consider three 1,2,3 selenadiazole derivatives shown in Scheme 1. Compound 9c shown in Scheme 1 was synthesized. Compounds 9c-1 and 9c-2 are

hypothetical. Hypothetical compounds were determined to study the effect of electron donor and acceptor groups. Inhibition activities of these compounds were predicted quantum chemical parameters such as highest occupied molecular orbital energy ($E_{HOMO}$), the lowest unoccupied molecular orbital energy ($E_{LUMO}$), the energy gap ($\Delta E$), hardness ($\eta$), softness ($\sigma$), electronegativity ($\chi$), chemical potential ($\mu$), global molecular electrophilicity index ($\omega$), global molecular nucleophilicity index ($\varepsilon$), the electron accepting ($\omega^+$) and electron donating ($\omega^-$) powers. Frontier molecular orbitals and molecular electrostatic potential (MEP) maps were discussed. Inhibition efficiencies were evaluated by molecular docking studies with the target protein PDB ID = 1M17 corresponding to the MCF-7 tumor cell line.
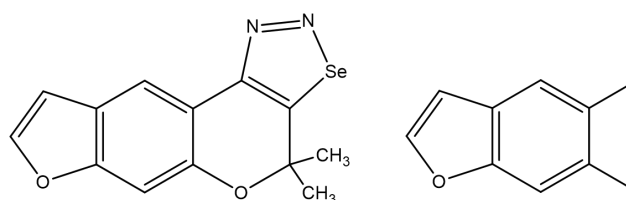


**Scheme 1.** 1,2,3-selendizole structure

## 2. THEORY AND COMPUTATIONAL DETAILS

GaussView 6.0.16 [9], Gaussian16 IA32W-G16RevB.01, Gaussian09 AS64L-G09RevD.01[10], ChemDraw were used for 9c, 9c-1 and 9c-2 calculations. Conceptual Density Functional Theory (CDFT) is a concept that offers simple equations in obtaining quantum chemical parameters. Some quantum chemical parameters such as the highest occupied molecular orbital energy ($E_{HOMO}$), the lowest unoccupied molecular orbital energy ($E_{LUMO}$), the energy gap ($\Delta E$), hardness ($\eta$), softness ($\sigma$), electronegativity ($\chi$), chemical potential ($\mu$), global molecular electrophilicity index ($\omega$), global molecular nucleophilicity index ($\varepsilon$), the electron accepting ($\omega^+$) and electron donating ($\omega^-$) powers are used to predict the

inhibition activities of the chemical species studied approximately [11,12]. HEX 8.0.0 program was used in docking studies [13].

The equations of the parameters used on the basis of the concept are as follows:

$$I = -E_{HOMO}$$

$$A = -E_{LUMO}$$

$$\eta = \frac{1}{2}\left[\frac{\partial^2 E}{\partial^2 N}\right]_{v(r)} = \frac{I-A}{2}$$

$$\langle\alpha\rangle = \frac{1}{3}\left[\alpha_{xx} + \alpha_{yy} + \alpha_{zz}\right] \quad \sigma = \frac{1}{\eta}$$

$$\mu = -\chi = \left[\frac{\partial E}{\partial N}\right]_{v(r)} = -\left(\frac{I+A}{2}\right)$$

$$\omega = \frac{\chi^2}{2\eta}$$

$$\varepsilon = \frac{1}{\omega}$$

$$\omega^+ = \frac{(I+3A)^2}{16(I-A)}$$

$$\omega^- = \frac{(3I+A)^2}{16(I-A)}$$

## 3. RESULTS AND DISCUSSION

### 3.1. Optimized Structure

Molecular structure of 9c, 9c-1 and 9c-2 were drawn using GaussView 6.0.16. The related calculations by using B3LYP method with 6-31G+(d) basis sets in gas phase were obtained at Gaussian16 IA32W-G16RevB.01, Gaussian09 AS64L-G09RevD.01. The obtained optimized structures of 9c, 9c-1 and 9c-2 are given Figure 1.
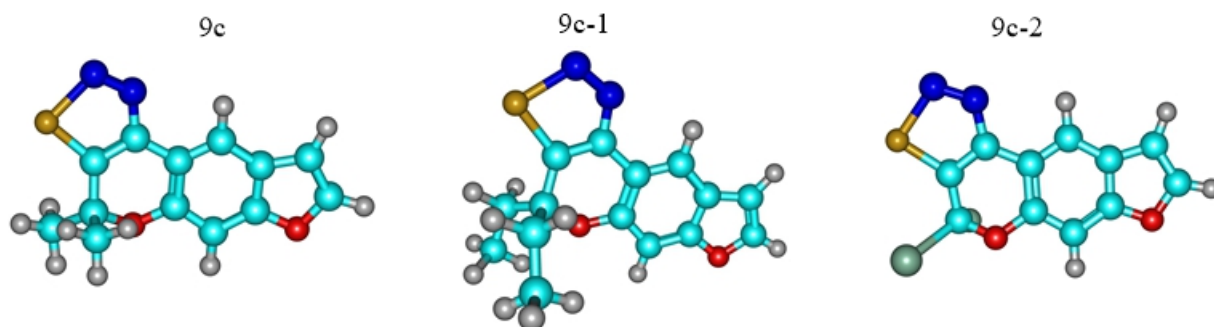


**Figure 1.** Optimized structures of 9c, 9c-1 and 9c-2

## 3.2. Molecular reactivity

Quantum chemical parameters were investigated to the theoretical inhibition activity of compound 9c, whose inhibition performance was investigated experimentally, and to predict the inhibition effect of the hypothetical 9c-1 and 9c-2 compound. A DFT study was implanted to establish a link between the electronic structures of the studied compounds and their inhibition efficiency. For this purpose, quantum chemical parameters for 9c, 9c-1 and 9c-2 were calculated in gas phase using the B3LYP method and the 6-31G+(d) basis set. The parameters examined in the gas phase using the B3LYP/6-31G+(d) level are given in Table 1.

**Table 1.** The calculated quantum chemical descriptors for the 9c, 9c-1 and 9c-2.

| Compound | 9c | 9c-1 | 9c-2 |
|---|---|---|---|
| $E_{HOMO}$ (eV) | -5.9436 | -5.8875 | -6.5920 |
| $E_{LUMO}$ (eV) | -2.1130 | -2.0556 | -2.7791 |
| $\Delta E$ (eV) | 3.8306 | 3.8319 | 3.8129 |
| $\eta$ (eV) | 1.9153 | 1.9160 | 1.9064 |
| $\sigma$ (eV$^{-1}$) | 0.5221 | 0.5219 | 0.5245 |
| $\chi$ (eV) | 4.0283 | 3.9715 | 4.6856 |
| $\mu$ (eV$^{-1}$) | -4.0283 | -3.9715 | -4.6856 |
| $\omega$ | 4.2362 | 4.1162 | 5.7580 |
| $\varepsilon$ | 0.2361 | 0.2429 | 0.1737 |
| $\omega^{+}$ | 1.5864 | 1.5425 | 2.1132 |
| $\omega^{-}$ | 6.490 | 6.341 | 8.339 |

The molecular reactivity descriptors obtained in the gas phase at the B3LYP/6-31G+(d) level are presented in Table 1. The anti-cancer activities of molecules can be determined using theoretical predictions provided by quantum chemical parameters. The first important parameter is HOMO's energy. If the energy of the HOMO is high, the electrons in the HOMO move more easily. The greater the electron mobility, the greater the inhibition efficiency of the molecules. LUMO energy values are an indicator of the electron uptake capacity. The lower the LUMO energy, the higher the inhibition efficiency. In addition, the energy gap of a molecule is equal to the difference of $\Delta E$, LUMO and HOMO energies. In addition, the energy gap of a molecule is equal to the difference of $\Delta E$, LUMO and HOMO energies. This parameter is the important parameter used to estimate the reactivity property. Decreasing values of $\Delta E$ mean more anti-cancer activity. Hardness and softness indicate the ability to polarize and interact. Normally, the higher the softness value and the lower the hardness value, the higher the inhibition efficiency. Chemical potential and electronegativity parameters provide vital information in determining the properties of the inhibitor. According to Sanderson's electronegativity balancing principle, the smaller the difference in electronegativity between the cancer protein structure and the inhibitor, the higher the inhibitor reactivity. For chemical potential, the opposite is expected, it can be said that the inhibition efficiency increases with low electronegativity and high chemical potential. Electrophilicity ($\omega$) and nucleophilicity ($\varepsilon$) indices are also very important for chemical reactivity prediction. If the electrophilicity ($\omega$) index is low, it behaves as a good nucleophile if it has a good electrophilicity and if the nucleophilicity ($\varepsilon$) index is high. The quantum chemical parameters $\omega^{+}$ and $\omega^{-}$ are the parameters representing electron acceptance and electron donation power, respectively. Among these parameters, increasing the $\omega^{-}$ value and decreasing the $\omega^{+}$ value increases the inhibition efficiency of chemical species. In the light of these generalizations, the binding of ethyl groups (9c-1) instead of methyl groups in compound 9c decreases the inhibition efficiency, while the binding of chlorine groups (9c-2) increases the inhibition efficiency.

As a result, the order of inhibition efficiency obtained at B3LYP/6-31+G(d) level in gas phase for the examined compounds is given as follow:

$$9c\text{-}2 > 9c > 9c\text{-}1$$

### 3.3. Frontier molecular orbitals

Frontier molecular orbitals include the highest occupied molecular orbital (HOMO) and the lowest empty molecular orbital (LUMO). With the help of the HOMO and LUMO molecular orbitals, the reactive sites within the inhibitor compounds could be predicted. In this regard,

frontier molecular orbital shapes of 9c, 9c-1 and 9c-2 at B3LYP/6-31+G(d) level are shown in Figure 2.
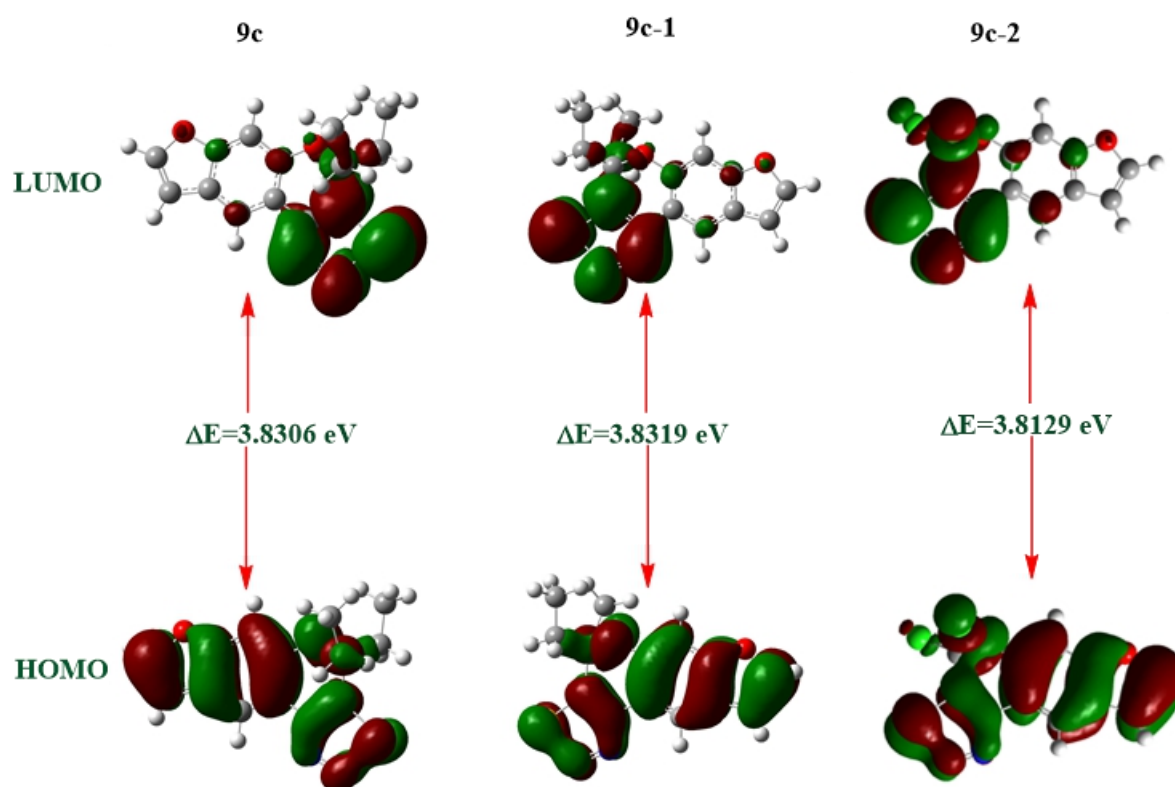


**Figure 2.** Frontier molecular orbital scheme.

As seen in Figure 2, in the 9c molecule, the HOMO is localized on the π molecular orbitals. Both the positive and negative lobes of carbon bonded to oxygen in the 9c molecule are larger than that of any other atom. The LUMO in the 9c molecule localized on the aromatic ring that contains the 1,2,3 selendiazole. In the 9c-1 molecule, the HOMO is localized on the 5-membered aromatic ring containing oxygen atom. The positive and negative lobes of the carbon directly attached to the oxygen atom are larger than any other atom. In the 9c-1 molecule, the LUMO is localized around the selenium atom. In the 9c-2 molecule, the HOMO is localized on the same orbitals as that of the 9c and 9c-1 molecules. Which is the five-membered ring containing the oxygen atom. In the 9c-2 molecule, the carbon attached directly to the oxygen atom possess both the positive and negative larger lobes than any other atom in the molecule. The LUMO on the 9c-2 molecule is localized on the aromatic ring congaing 1,2,3-selendiazole in which the selenium atom has larger lobes.
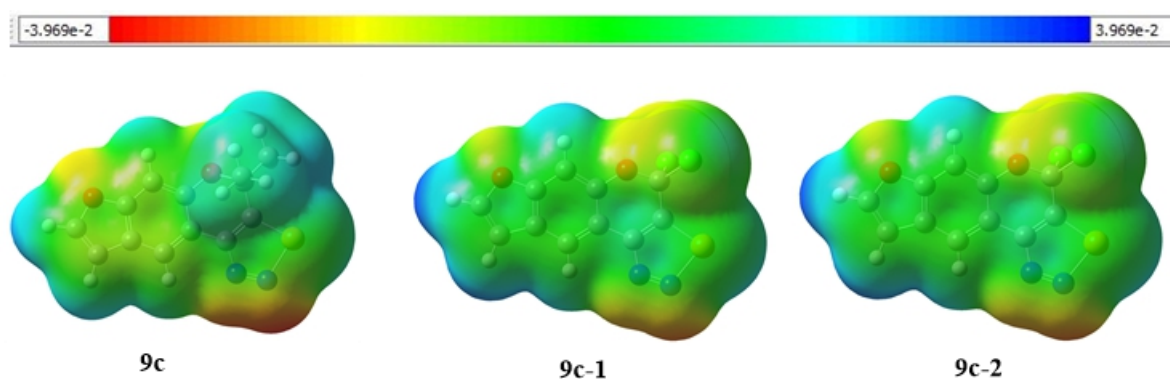


**Figure 3.** MEP maps of investigated 1,2,3-selendiazole derivatives
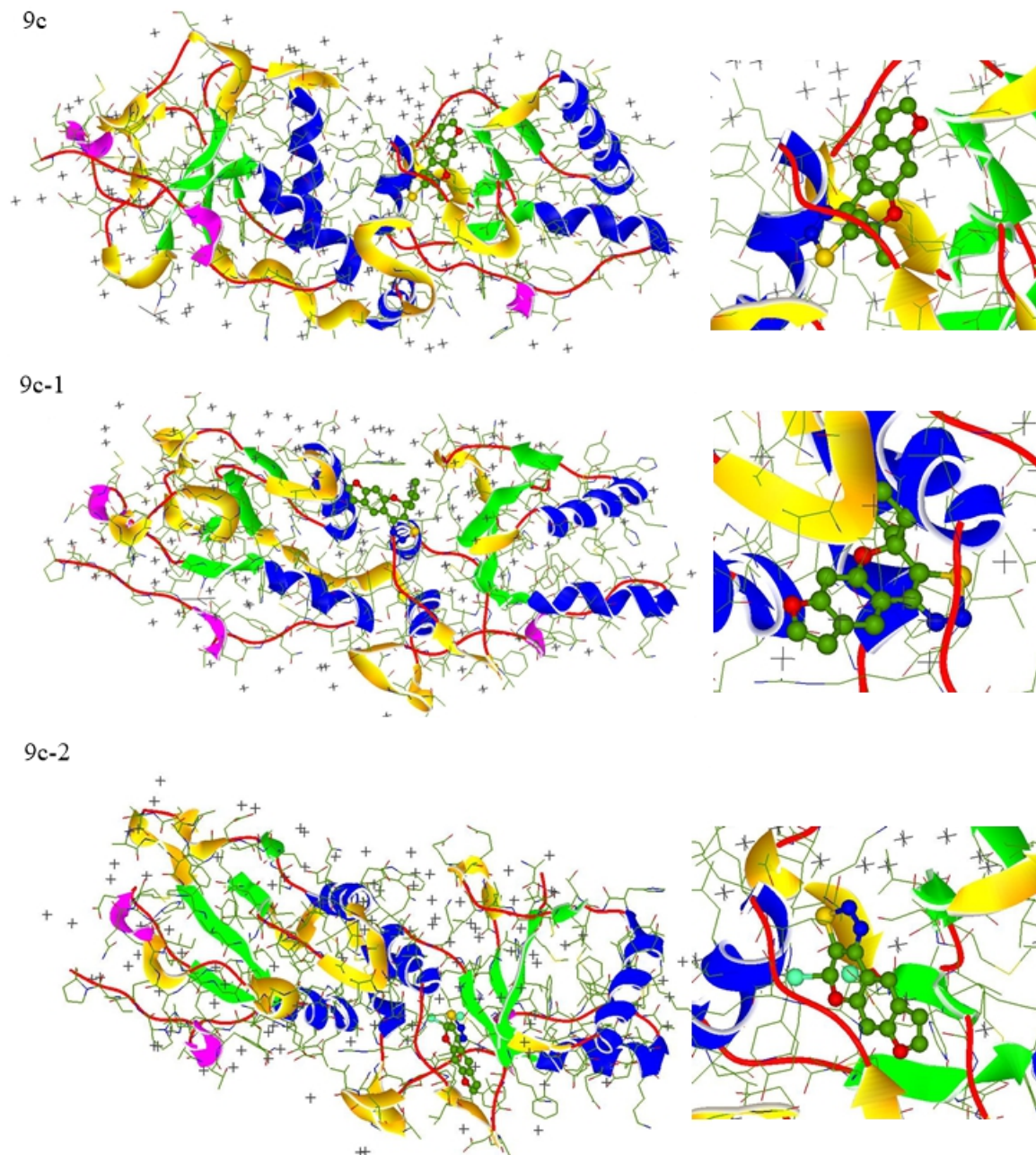
**Figure 4.** Binding poses of 1,2,3-selenediazole derivatives and 1JNX target protein.

## 3.1. Molecular electrostatic potential (MEP) maps

With the molecular electrostatic potential maps, the active sites on molecules can be determined. It also provides vital information which helps to predict the corrosion mechanism of a molecule. They also enable us to visualize the size and shape of molecules. The electrophilic and nucleophilic positions can also be identified using MEP [14-17].

In MEP maps, the electrophilic reactivity is shown in the positive (blue) region and nucleophilicity in the negative (red) region. According to Figure 3, the blue colored regions are electrophilic and the red colored regions are the nucleophilic region. Blue regions prefer to coordinate with the electron-rich positions of any chemical species. The red-colored regions prefer to coordinate with

the electron-poor positions of any chemical species. In 9c, red regions are seen on oxygen and nitrogen atoms present in the 1,2,3-seledinazole ring. These regions are electrophilic making them electron-rich. In 9c-1, the electrophilic regions are the same with that of 9c molecule. In 9c-2, the red regions are seen on the nitrogen atoms, the oxygen neighboring the chlorine atoms and the other oxygen neighboring benzene ring at the terminal. This situation gave results that are compatible with the contour diagrams of HOMO and LUMO molecular orbitals that were obtained in the frontier molecular orbitals segment.

## 3.2. Molecular docking

In recent years, molecular docking studies have attracted great attention in computational studies. The binding energy between the molecules examined by

molecular docking and the target protein determined according to the cancer type can be correlated with the experimentally determined semi-maximal inhibitor concentration (IC$_{50}$). The target protein is the protein corresponding to the experimentally selected cancer cell and is obtained from the protein database [18]. In this study, the selenium compounds investigated were placed against the MCF-7 breast cancer cell line. The target protein (PDB ID: 1JNX) representing the MCF-7 breast cancer cell line was designated. 1JNX is breast cancer-associated protein and represents the BRCA1 region of the BRCT crystal structure. BRCA1 is the region containing approximately 90-100 amino acid sequence repeats of the C-terminal region. The C-terminal region in BRCA1 occurs with mutations that cause early onset breast cancer. This area is very important for tumor suppression. Amino acid repeats in BRCT are very important in DNA repair [19]. In this study, 9c, 9c-1, and 9c-2 selenium compounds were docked against PDB ID: 1JNX and their docking poses are given in Figure 4.

According to docking results, binding energies between 9c, 9c-1 and 9c-2 and 1JNX target protein were calculated as -215.88, -198.3 and -234.25 kcal/mol, respectively. This situation may be associated with the change in inhibition efficiency in the presence of electron-attracting and electron donor groups. A similar situation is consistent with the results obtained with quantum chemical parameters.

## 4. CONCLUSION

Three 1,2,3-selendiazole derivative compounds (9c, 9c-1 and 9c-2) were considered to investigate their inhibitory activity at the molecular scale. 9c is an experimentally synthesized compound. The ethyl (electron donor) and chlorine (electron acceptor) groups were added to compound 9c to predict compounds 9c-1 and 9c-2, respectively. The change in inhibition activities was investigated by adding electron donor and acceptor groups on the synthesized compound. From the optimized geometries obtained, it was concluded that the molecules are planar. Inhibition efficiencies were compared with quantum chemical parameters. It was predicted by quantum chemical parameters that the inhibition efficiency of the electron donor group decreased and the inhibition efficiency of the electron withdrawing group increased. The positions of the electron donor and acceptor lobes are explained with the Frontier molecules orbitals diagrams. Electrophilic and nucleophilic regions were determined with MEP maps. In molecular docking studies, binding energies between 9c, 9c-1 and 9c-2 and 1JNX target protein were found as -215.88, -198.3 and -234.25 kcal/mol, respectively. These results were found to be quite compatible with the order of inhibition efficiency predicted in quantum chemical parameters.

## REFERENCES

[1]  W. Fischer, J. Chem. Educ. 78 (2001) 1333.

[2]  C. Thiry, A. Ruttens, L. De Temmerman, Y.J. Schneider, L. Pussemier, Current knowledge in species-related bioavailability of seleium in food, Food Chem. 130 (4) (2012) 767–784.

[3]  S. Misra, M. Boylan, A. Selvam, J.E. Spallholz, M. Björnstedt, Redox-active selenium compounds—from toxicity and cell death to cancer treatment, Nutrients 7 (5) (2015) 3536–3556.

[4]  T. Chen, W. Zheng, Y.S. Wong, F. Yang, Mitochondria-mediated apoptosis in human breast carcinoma MCF-7 cells induced by a novel selenadiazole derivative, Biomed. Pharmacother. 62 (2008) 77–84.

[5]  T. Chen, Y.S. Wong, W. Zheng, J. Liu, Caspase- and p53-dependent apoptosis in breast carcinoma cells induced by a synthetic selenadiazole derivative, Chem. Biol. Interact. 180 (2009) 54–60.

[6]  C. Sanmartin, D. Plano, J.A. Palop, Selenium compounds and apoptotic modulation: a new perspective in cancer therapy, Mini Rev. Med. Chem. 8 (2008) 1020–1031.

[7]  W. Dorr, Effects of selenium on radiation responses of tumor cells and tissue, Strahlenther. Onkol. 182 (2006) 693–695.

[8]  Atta, S. M. S., Farrag, D. S., Sweed, A. M., & Abdel-Rahman, A. H. (2010). Preparation of new polycyclic compounds derived from benzofurans and furochromones. An approach to novel 1, 2, 3-thia-, and selena-diazolofurochromones of anticipated antitumor activities. European journal of medicinal chemistry, 45(11), 4920-4927.

[9]  Dennington II, R. D., Keith, T. A., & Millam, J. M. (2009). GaussView 5.0, Wallingford, CT.

[10]  Gaussian09, R. (2009). 02, MJ Frisch, GW Trucks, HB Schlegel, GE Scuseria, MA Robb, JR Cheeseman, G. Scalmani in no. 3 Gaussian. Inc., Wallingford, 4

[11]  EL AATIAOUI, A., Koudad, M., Chelfi, T., ERKAN, S., Azzouzi, M., Aouniti, A., ... & Oussaid, A. Experimental and theoretical study of new Schiff bases based on imidazo (1, 2-a) pyridine as corrosion inhibitor of mild steel in 1M HCl. Journal of Molecular Structure, 1226, 129372.

[12]  Al-Otaibi, J. S., Mary, Y. S., Mary, Y. S., Kaya, S., & Erkan, S. (2020). Spectral analysis and DFT investigation of some benzopyran analogues and their

self-assemblies with graphene. Journal of Molecular Liquids, 317, 113924.

[13] Erkan, S., & Karakaş, D. (2019). DFT investigation and molecular docking studies on dinuclear metal carbonyls containing pyridyl ligands with alkyne unit. Chemical Papers, 73(10), 2387-2398.

[14] Kaya, S., Erkan, S., & Karakaş, D. (2020). Computational investigation of molecular structures, spectroscopic properties and antitumor-antibacterial activities of some Schiff bases. Spectrochimica Acta Part A: Molecular and Biomolecular Spectroscopy, 244, 118829.

[15] Ceylan, M., Erkan, S., Yaglioglu, A. S., Akdogan Uremis, N., & Koç, E. (2020). Antiproliferative Evaluation of Some 2-[2-(2-Phenylethenyl)-cyclopent-3-en-1-yl]-1, 3-benzothiazoles: DFT and Molecular Docking Study. Chemistry & Biodiversity, 17(4), e1900675.

[16] Erkan, S., & Karakaş, D. (2020). A theoretical study on cyclometalated iridium (III) complexes by using a density functional theory.

[17] Erkan, S. (2019). Activity of the rocuronium molecule and its derivatives: A theoretical calculation. Journal of Molecular Structure, 1189, 257-264.

[18] ERKAN, S. (2018). Structural, Spectroscopic and Anti-cancer Properties of Hydroxy-and Sulfonamide-Azobenzene Platinum (II) Complexes: DFT and Molecular Docking Studies. Cumhuriyet Science Journal, 39(4), 1036-1051.

[19] Kaya, S., Erkan, S., & Karakaş, D. (2021). Computational investigation of molecular structures, spectroscopic properties and antitumor-antibacterial activities of some Schiff bases. Spectrochimica Acta Part A: Molecular and Biomolecular Spectroscopy, 244, 118829.